VARIABILITY OF DUST AEROSOL PARTICLE SIZE AT GALE CRATER USING MASTCAM AND REMS UV MEASUREMENTS

A. De Vicente-Retortillo, Departamento de Física de la Tierra, Astronomía y Astrofísica II, Universidad Complutense de Madrid, Madrid, Spain (*avicenteretortillo@gmail.com*), **G. M. Martínez**, Department of Climate and Space Sciences and Engineering, University of Michigan, Ann Arbor, MI, USA, **N. O. Renno**, Department of Climate and Space Sciences and Engineering, University of Michigan, Ann Arbor, MI, USA, **M. T. Lemmon**, Department of Atmospheric Sciences, Texas A&M University, College Station, TX 77843-3150, USA, **M. de la Torre-Juárez**, Jet Propulsion Laboratory, California Institute of Technology, 4800 Oak Grove Drive, Pasadena, CA 91109, USA.

Introduction: Dust aerosols are ubiquitous in the Martian atmosphere and interact strongly with solar and thermal radiation [*1*]. In particular, dust particle size determines the ratio between the atmospheric opacity at short and long wavelengths, affecting the atmospheric heating rates and thus playing a role in the atmospheric thermal and dynamical structure ([*2*], [*3*]).

The Rover Environmental Monitoring Station (REMS) onboard the Mars Science Laboratory (MSL) *Curiosity* rover carries a UV sensor (UVS) that has been measuring solar radiation in six bands between 200 and 380 nm for more than two Martian years (MY) [*4*].

Here we present a novel methodology to determine dust particle sizes using REMS/UVS measurements in combination with Mastcam retrievals of atmospheric opacity. We calculate the dust particle size and show its seasonal and interannual evolution during the first 1413 sols of the MSL mission. In addition, we calculate the correlation between the dust particle size and the atmospheric opacity [*5*].

Methodology: We use the photodiode output currents (TELRDR products) and the ancillary (ADR) data of the REMS/UVS UVE channel, and the values of the atmospheric opacity at 880 nm obtained from Mastcam observations. We select the UVE channel because it matches the 320 nm UV channel of the Mars Color Imager (MARCI) on board the Mars Reconnaissance Orbiter (MRO), from which the refractive indices that we use in the calculations of the radiative properties of the dust particles were obtained ([*4*], [*6*]).

We analyze measurements on sols when the Sun was temporally blocked by either the masthead or the mast of the rover because the behavior of the photodiode output current during those shadow events depends on the dust aerosol particle size. We retain those measurements in which the masthead remains in its most typical position (azimuth ~ -179º and elevation ~ 43º) in order to accurately calculate the fraction of the incoming radiation blocked by the mast and masthead of the rover.

Then, we simulate the radiance at the surface during the shadow events using our Monte-Carlo radiative transfer scheme. The UV fluxes obtained using this scheme are in very good agreement with those using our model COMIMART, which also considers updated aerosol radiative properties and has been validated using DISORT [*7*].

The simulated radiance depends on the dust opacity and radiative properties (single scattering albedo and scattering phase function). In turn, these two radiative properties depend on the refractive indices and on the shape and size distribution of the particles. We calculate these parameters using a T-Matrix code ([*8*], [*9*]). For these calculations, we have assumed that particles are cylinders with diameter-to-length ratio D/L = 1 [*10*] which follow a power law distribution ([*9*], [*11*], [*12*]) with a typical effective variance of 0.3 ([*7*] and references herein).

We calculate the radiances for different combinations of opacities and particle sizes. Then we simulate the photodiode output current for each combination using our empirical model, which considers the tilt and orientation of the rover, the angular response of the photodiode (shown in Figure 1), and the region of the FOV blocked by the masthead and by the mast.

By analyzing the sensitivity of the results and the goodness of the fits we select the events with the highest confidence and we retrieve the dust particle size.

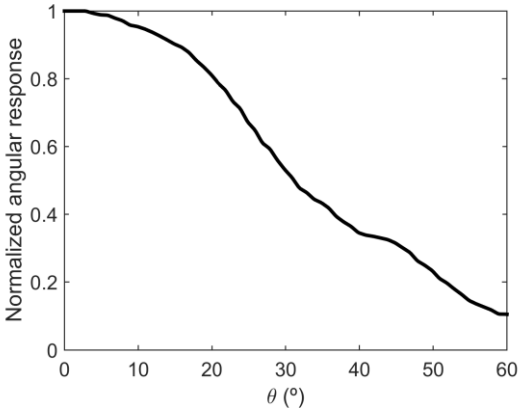

Figure 1. *Empirically calculated angular response of the UVE channel as a function of zenith angle [*5*].*

Results: The top panel of Figure 2 shows the seasonal and interannual variability of the dust particle effective radius as a function of solar longitude for MY 31 (blue), 32 (black) and 33 (red). The variability of averaged opacity is shown for the

sake of comparison in the bottom panel.

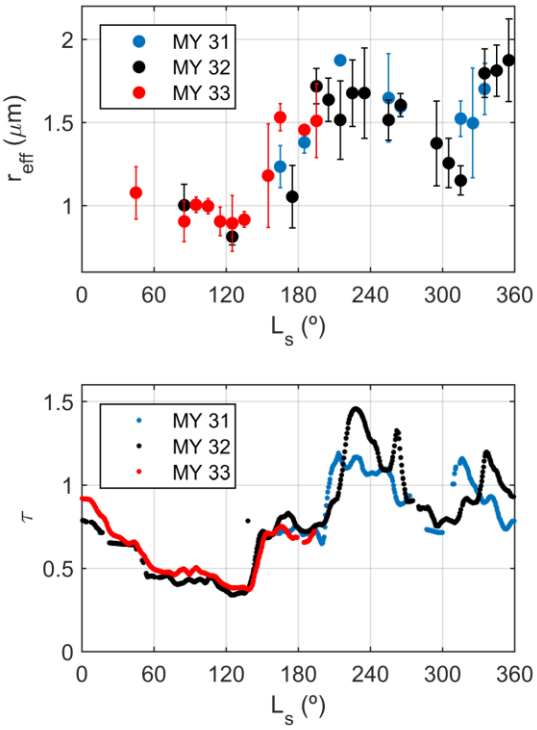

Figure 2. *Seasonal and interannual evolution of the dust aerosol particle size (top) and atmospheric opacity (bottom) at the MSL landing site.*

Seasonal and interannual variability: Dust particle size shows a significant seasonal variability, with values of the effective radius that range from ~0.8 to ~2 μm. During the aphelion season (L_s = 0º – 180º), the dust particle size is relatively small and the intraseasonal variability is small, while during the perihelion season (L_s = 180º – 360º) the effective radii are larger and the intraseasonal variability is significant.

On MY 31, Mastcam and REMS/UVS measurements started around L_s = 155º, when we calculate values of the dust particle size around 1.2 – 1.4 μm (Figure 2, top). Following the sudden increase in the opacity occurred at L_s = 208º (Figure 2, bottom), the dust particle size increased significantly, reaching values around 2 μm. At the end of this period of high opacity, at L_s ~ 255º, the dust particle size was relatively large and showed values around 1.6 μm. During the second period of high opacities, between L_s = 300º – 350º, dust particle sizes were moderately large, with values above 1.5 μm.

On MY 32, the dust particle size showed the annual minimum at L_s = 125º (Figure 2, top), coinciding with the time of the year when the atmospheric opacity was the lowest (Figure 2, bottom). During the main dust event of this year around L_s = 225º, the effective radius was relatively high, with values around 1.7 μm. At L_s ~ 300º, dust particle sizes decreased to ~1.2 μm, coinciding with the local minimum in atmospheric opacity between the main episode of high opacity and the one that peaked at L_s = 335º. Effective radii increased again during the latter dust event.

On MY 33, we obtained a better coverage during the low atmospheric opacity season (L_s = 60º – 140º) than on the previous year. Results during this time show that the particle size typically remained within the range 0.8 – 1.0 μm, with the atmospheric opacity showing the annual minimum values. During the transition towards the dusty season starting at L_s ~150º, there was an increase in the particle radius, which coincided with an increase in atmospheric opacity.

From an interannual perspective, we find differences between the aphelion and the perihelion seasons. During the low atmospheric opacity season, dust particle sizes on MY 32 and MY 33 are similar. In contrast, during the aphelion season the interannual variability is larger. As an example, dust particle sizes values on MY 31 between L_s = 300º – 350º were larger than on MY 32 during the first half, whereas the opposite behavior is observed at L_s ~335º.

Correlations with dust opacity: In the previous subsection we have shown that dust particle size and atmospheric opacity follow similar seasonal trends. In particular, when the atmospheric opacity is relatively high ($\tau > 1$), dust particle size is above 1.5 μm, whereas when the atmospheric opacity is low ($\tau < 0.5$), the effective radius is below 1 μm.

Figure 3 shows our calculated effective radii as a function of Mastcam atmospheric opacity. The correlation between the two variables is apparent (R^2 = 0.67), especially for opacities below one. This behavior is physically consistent because dust particle sizes are expected to be smaller during the low atmospheric opacity season due to the deposition of larger particles that were lifted during the dust events.

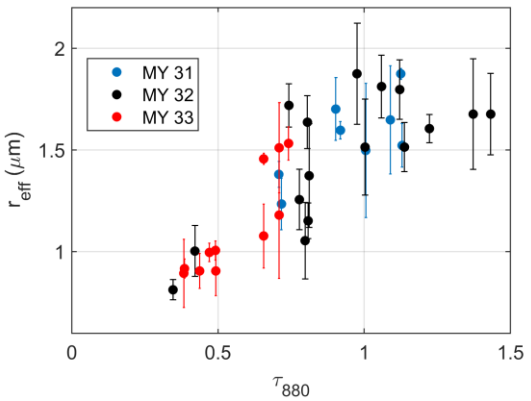

Figure 3. *Dust aerosol particle size at the MSL landing site as a function of opacity at 880 nm.*

Discussion: The values and seasonal variability of the dust aerosol particle size are consistent with those obtained at the locations of the Mars Exploration Rovers (MER) *Spirit* and *Opportunity* using the ratio between dust opacity measured at 9 μm by the Mini Thermal Emission Spectrometer (Mini-TES) and the opacity measured at 880 nm by Pancam [*13*]. Particle sizes at both locations were virtually always in the range between 0.7 and 2.1 μm. The lowest values were found during the low atmospheric opacity season while the highest sizes generally occurred when the opacity peaked, in very good agreement with our results at the *Curiosity* location.

Finally, the correlation between atmospheric opacity and dust particle size is particularly notorious when the atmospheric opacity is low, while it becomes less apparent when the atmospheric opacity is high. This is also in agreement with the results from *Spirit* observations during MY 27, which show values above 2 μm for the peak at L_s = 135º - 150º and around 1.4 μm at L_s = 225º - 240º [*13*]. This suggests that these locations are affected by events of high aerosol content originated at different regions.

Acknowledgments: This study has been partially supported by the research projects AYA2011-29967-C05-02 and CGL2011-25327, funded by the Spanish Ministry of Economy and Competitiveness. Also the author A. Vicente-Retortillo wishes to acknowledge the Ministry FPI scholarship (BES-2012-059241) for the financial support and training. We thank the MSL and REMS Teams for supporting this investigation.

Bibliography:

[*1*] Read, P.L., and S.R. Lewis. *The Martian climate revisited: atmosphere and environment of a desert planet*, Springer-Verlag, Berlin, 2004.

[*2*] Madeleine, J.-B. et al. Revisiting the radiative impact of dust on Mars using the LMD Global Climate Model. *J. Geophys. Res*., 116, E11010, 2011.

[*3*] Medvedev, A. S., Kuroda, T., and Hartogh, P. Influence of dust on the dynamics of the martian atmosphere above the first scale height. *Aeolian Res.*, 3(2), 145-156, 2011.

[*4*] Gómez-Elvira, J. et al. REMS: the environmental sensor suite for the Mars Science Laboratory rover. *Space Sci. Rev.*, 170 (1-4), 583-640, 2012.

[*5*] Vicente-Retortillo et al. Variability of dust aerosol particle size at Gale Crater from REMS/UVS and Mastcam measurements. *Geophys. Res. Lett.* (in preparation).

[*6*] Wolff, M. J. et al. Ultraviolet dust aerosol properties as observed by MARCI. *Icarus*, 208 (1), 143-155, 2010.

[*7*] Vicente-Retortillo, A. et al. A model to calculate solar radiation fluxes on the Martian surface. *J. Space Weather Space Clim.*, 5, A33, 2015.

[*8*] http://www.giss.nasa.gov/staff/mmishchenko/t_matrix.html

[*9*] Mishchenko, M. I., and Travis, L. D. Capabilities and limitations of a current FORTRAN implementation of the T-matrix method for randomly oriented, rotationally symmetric scatterers. *J. Quant. Spectrosc. Radiat. Transfer*, 60(3), 309-324., 1998.

[*10*] Wolff, M. J. et al. Wavelength dependence of dust aerosol single scattering albedo as observed by the Compact Reconnaissance Imaging Spectrometer. *J. Geophys. Res.*, 114, E00D04, 2009.

[*11*] Mishchenko, M. I., and Travis, L. D. Light scattering by polydispersions of randomly oriented spheroids with sizes comparable to wavelengths of observation. *Appl. Opt.*, 33(30), 7206-7225, 1994.

[*12*] Hansen, J. E., and Travis, L. D. Light scattering in planetary atmospheres. *Space Sci. Rev.*, 16, 527-610, 1974.

[*13*] Lemmon, M. T. et al. Dust aerosol, clouds, and the atmospheric optical depth record over 5 Mars years of the Mars Exploration Rover mission. *Icarus*, 251, 96-111, 2015.